molecular pharmaceutics

Article

pubs.acs.org/molecularpharmaceutics

Translocator Protein Ligand–PLGA Conjugated Nanoparticles for 5-Fluorouracil Delivery to Glioma Cancer Cells

Valentino Laquintana,*[,†] Nunzio Denora,*[,†] Antonio Lopalco,[†] Angela Lopedota,[†] Annalisa Cutrignelli,[†] Francesco Massimo Lasorsa,[‡] Giulia Agostino,[§] and Massimo Franco[†]

[†]Dipartimento di Farmacia-Scienze del Farmaco, Università degli Studi di Bari "Aldo Moro", via Orabona 4, 70125 Bari, Italy

[‡]CNR Institute of Biomembranes and Bioenergetics, via Amendola, 165/a, 70126 Bari, Italy

[§]Dipartimento di Bioscienze, Biotecnologie e Biofarmaceutica, Università degli Studi di Bari "Aldo Moro", via Orabona 4, 70125 Bari, Italy

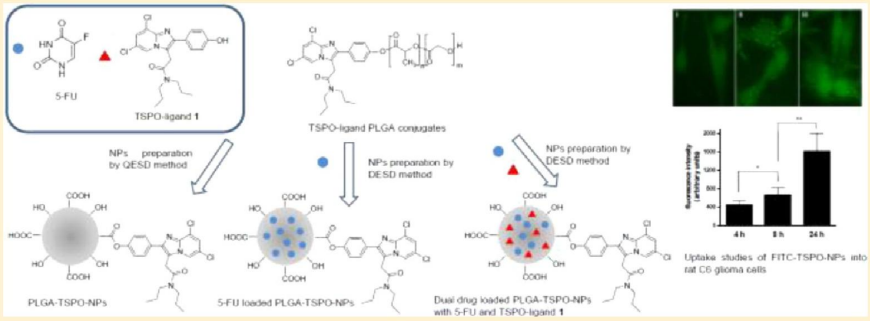

ABSTRACT: Translocator protein 18 kDa (TSPO) is a promising target for molecular imaging and for targeted drug delivery to tumors overexpressing TSPO. In our previous work, new macromolecular conjugates with a high affinity and selectivity for TSPO were prepared by conjugating the biodegradable poly(D,L-lactic-*co*-glycolic acid) (PLGA) polymer with two potent and selective TSPO ligands, namely, compounds **1** and **2**. Based on this, nanoparticle delivery systems (NPs), employing TSPO ligand–PLGA conjugated (PLGA–TSPO) polymers, were prepared. Furthermore, to evaluate the ability of the new NPs to be used as a drug delivery systems for anticancer therapy, PLGA–TSPO NPs were loaded with 5-fluorouracil (5-FU), chosen as a model hydrophilic anticancer drug. The main goal of this work was to investigate the synergistic potential of using NP conjugates PLGA–TSPO, TSPO ligands being pro-apoptotic agents, to simultaneously deliver a cytotoxic anticancer drug. To better highlight the occurrence of synergistic effects, dual drug loaded PLGA NPs (PLGA NPs/5-FU/**1**) and dual drug loaded PLGA–TSPO NPs (PLGA–TSPO NPs/5-FU/**1**), with 5-FU and TSPO ligand **1** physically incorporated together, were also prepared and characterized. The particle size and size distribution, surface morphology, and drug encapsulation efficiency, as well as the drug release kinetics, were investigated. *In vitro* cytotoxicity studies were carried out on C6 glioma cells overexpressing TSPO, and to evaluate the potential uptake of these nanoparticulate systems, the internalization of fluorescent labeled PLGA–TSPO NPs (FITC–PLGA–TSPO NPs) was also investigated by fluorescence microscopy. Results demonstrated that PLGA–TSPO NPs/5-FU and dual drug loaded PLGA NPs/5-FU/**1** and PLGA–TSPO NPs/5-FU/**1** could significantly enhance toxicity against human cancer cells due to the synergistic effect of the TSPO ligand **1** with the anticancer drug 5-FU.

KEYWORDS: *translocator protein, 5-fluorouracil, poly(D,L-lactide-co-glycolide), conjugates, nanoparticles, intracellular drug delivery*

■ INTRODUCTION

Translocator protein 18 kDa (TSPO), previously known as peripheral-type benzodiazepine receptor (PBR),[1] has been identified as a new class of mitochondrial proteins and is an emerging target for molecular imaging and for targeted drug delivery to tumors overexpressing TSPO.[2,3] TSPO forms a multimeric complex with the 32 kDa voltage-dependent anion channel (VDAC) and with the 30 kDa adenine nucleotide carrier (ANC) in the outer mitochondrial membrane.[4] This trimeric complex is a key component of the mitochondrial permeability transitional pore (MPTP), which is involved in a wide number of biological processes including cell growth and proliferation, heme biosynthesis, calcium flow, chemotaxis and cellular immunity, steroidogenesis, mitochondrial respiration, and apoptosis.[5−7] TSPO overexpression has been shown in many tumor types, including brain, breast, colorectal, prostate, and ovarian cancers, as well as astrocytomas, hepatocellular, and endometrial carcinomas.[8−10]

Received: September 5, 2013
Revised: January 10, 2014
Accepted: January 11, 2014
Published: January 11, 2014

Endogenous ligands for the TSPO are the diazepam-binding inhibitor (DBI) porphyrins, while different structural classes of synthetic compounds such as 2-phenylindole-3-acetamides (FGIN),[11] isoquinoline-derivatives (PK 11195),[12] benzodiazepines (Ro-5-4864),[13] *N*-phenoxyphenyl-*N*-isopropoxybenzyl-acetamides (DAA1097),[14] and 2-phenyl-imidazo[1,2-*a*]pyridine acetamides have been identified as TSPO ligands.[15]

For targeted release of anticancer drugs, TSPO-ligands have been extensively explored,[16−20] and they have been used as diagnostic imaging agents as well.[21−24] Moreover, recently we have prepared new macromolecular conjugates with high affinity for the TSPO, by conjugation of the biodegradable poly(D,L-lactic-*co*-glycolic acid) (PLGA) polymers (TSPO ligand-PLGA conjugates **4**−**6**, in Chart 1) with 2-phenyl-imidazo[1,2-*a*]pyridine acetamides (TSPO-ligand **1** and **2**, in Chart 1).[25] These TSPO ligands possess high affinity (in nanomolar concentration) and selectivity toward the mitochondrial protein.[16] Moreover, the presence in the structure of appropriate functional groups allows to obtain prodrugs,[26] bioconjugates, and targeted drug delivery systems.[27] In particular, TSPO ligands **1** and **2** contain a phenolic and an amino group, respectively, useful for their further conjugation. Finally, these ligands, at appropriate concentrations, are able to induce apoptosis in rat C6 glioma cells.[25]

The promising results of the above-mentioned work led us to develop new nanoparticulate (NP) delivery system formulations, potentially useful in the treatment of cancer. In particular, starting from these TSPO-ligand−PLGA conjugates **4**−**6**, NPs containing the TSPO ligands **1** and **2** have been prepared (TSPO-ligand−PLGA conjugates NPs, PLGA−TSPO NPs), and TSPO ligand **1** loaded PLGA NPs/**1** were also prepared. Moreover biodegradable NPs made with PLGA alone **3** (PLGA NPs) were used as controls. Fluorescent NPs (FITC−PLGA−TSPO NPs and FITC−PLGA NPs), labeled with fluorescein isothiocyanate (FITC), also have been prepared starting from the TSPO ligand FITC−PLGA conjugate **7** and FITC−PLGA conjugate **8**, respectively (Chart 1).

PLGA−TSPO NPs, PLGA NPs, PLGA NPs/**1**, FITC−PLGA−TSPO NPs, and FITC−PLGA NPs were prepared by a *quasi*-emulsion solvent diffusion method (QESD). Furthermore, to ascertain the ability of the new NPs to be used as drug delivery system for anticancer therapy, PLGA−TSPO NPs and PLGA NPs were loaded with 5-fluorouracil (5-FU), chosen as a model hydrophilic cytotoxic anticancer drug. The 5-FU is a pyrimidine analogue used for the treatment of several malignancies such as colorectal and breast cancers. 5-FU shows a short half-life of a few minutes after intravenous injection (i.v.) and some dosing-related side effects.[28] Thus, to increase the therapeutic efficacy and safety of 5-FU, various drug delivery systems, including micro- and nanoparticles encapsulating 5-FU have been evaluated.[29−32] Recently, 5-FU loaded biodegradable microparticles have been implanted in the brain after resection of malignant gliomas.[32,33]

The main aim of this work was to investigate the feasibility of using NPs systems, formed with TSPO-ligand PLGA conjugates, to deliver the anticancer drug 5-FU into cancer cells in combination with TSPO-ligands as pro-apoptotic agents. This is to assess the potential synergistic effects of the TSPO ligand **1** on the activity of the cytotoxic drug. Thus to better highlight the occurrence of synergistic effects, dual drug loaded PLGA NPs (PLGA NPs/5-FU/**1**) and dual drug loaded PLGA−TSPO−**4a** NPs (PLGA−TSPO−**4a** NPs/5-FU/**1**), with 5-FU and TSPO ligand **1**, were prepared and characterized. In particular, 5-FU loaded PLGA NPs (PLGA NPs/5-FU), 5-FU loaded PLGA−TSPO NPs set (PLGA−TSPO NPs/5-FU), the dual drug loaded PLGA NPs/5-FU/**1** and PLGA−TSPO−**4a** NPs/5-FU/**1** were prepared by a double emulsion solvent diffusion technique (DESD).

The particle size and size distribution, surface morphology, thermal behavior, and drug encapsulation efficiency, as well as the *in vitro* drug release kinetics, were investigate. The cytotoxicity of empty PLGA−TSPO−**4a** NPs, PLGA-NPs/5-FU, PLGA−TSPO−**4a** NPs/5-FU, PLGA NPs/5-FU/**1**, and PLGA−TSPO−**4a** NPs/5-FU/**1** was investigated *in vitro* on rat C6 glioma cell line. Cellular up-take properties of these

Chart 1. Chemical Structures of TSPO Ligands 1 and 2, PLGA (3a−c) TSPO Ligand−PLGA Conjugates 4a,b, 5a,b, and 6, TSPO Ligand−FITC−PLGA Conjugate 7, and FITC−PLGA Conjugate 8

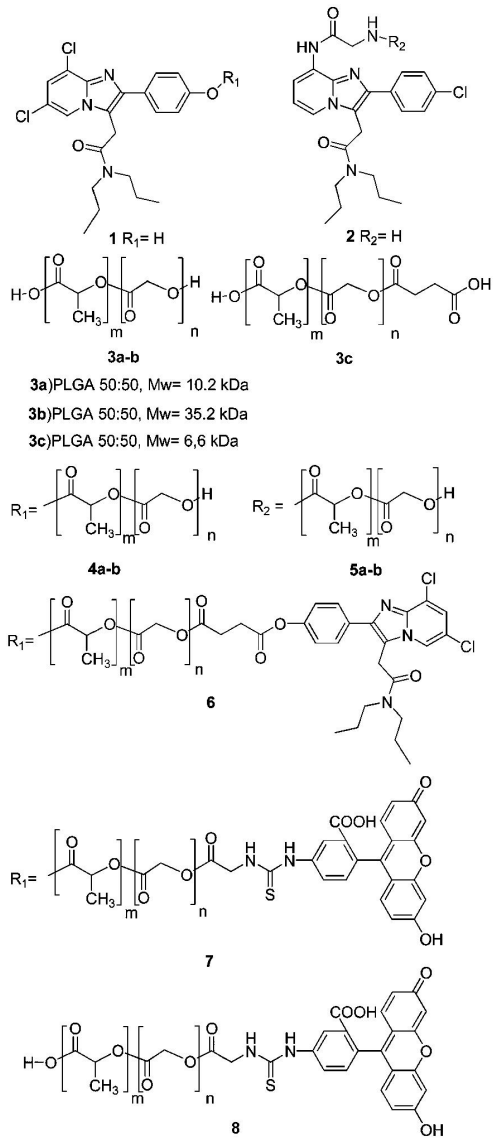

dx.doi.org/10.1021/mp400536z | *Mol. Pharmaceutics* 2014, 11, 859−871

nanoparticulate systems were also evaluated on rat C6 glioma cells using FITC-PLGA NPs.

■ MATERIALS AND METHODS

Materials. Poly(D,L-lactide-*co*-glicolide) (PLGA, Resomer RG502H, M_w = 10.2 kDa **3a**, and Resomer RG503H, M_w = 35,2 kDa, **3b**) having a lactic/glycolic acid molar ratio of 50/50 and a free hydroxyl- and carboxylic acid-group at its terminal ends were purchased from Boehringer-Ingelheim, Ingelheim am Rhein, Germany. Lutrol F68 (Poloxamer 188) was supplied from BASF (Germany). 5-Fluorouracil (5-FU) was purchased from Sigma-Aldrich (Milan, Italy). All other chemicals were of analytical grade.

The TSPO ligands *N*,*N*-di-*n*-propyl-[2-(6,8-dichloro-2-(4-hydroxyphenyl)imidazo[1,2-*a*]pyridin-3-yl)]acetamide **1**, PLGA conjugates **4**−**6**, and FITC-conjugated probes **7**−**8** were prepared according to synthetic procedures reported elsewhere.[25]

Apparatus. HPLC analyses were performed with a Waters Associates (Milford, MA, USA) model 1515 HPLC isocratic pump, a Symmetry C18 (4.6 × 150 mm, 5 μm) column, a Waters 2487 UV−vis detector, and the Breeze Software to analyze the chromatographic data. The mobile phase was a mixture of phosphate buffer solution (1 mM, pH 7.4) and methanol 40:60 (v/v) at a flow rate of 0.8 mL/min. The column effluent was monitored continuously by UV at 266 nm to assay for 5-FU. TSPO-ligand **1** loaded into the NPs was quantified using a mixture of water/methanol 30:70 (v/v) as eluent (0.8 mL/min) and a wavelength of 254 nm to monitor **1**.

Preparation of NPs. PLGA−TSPO-NPs set (PLGA−TSPO−**4a** NPs, PLGA−TSPO−**4b** NPs, PLGA−TSPO−**5a** NPs, PLGA−TSPO−**5b** NPs, and PLGA−TSPO−**6** NPs) and PLGA NPs/**1** were prepared by a QESD technique.[34] PLGA−TSPO-NPs/5-FU set (PLGA−TSPO−**4a** NPs/5-FU, PLGA−TSPO−**4b** NPs/5-FU, PLGA−TSPO−**5a** NPs/5-FU, PLGA−TSPO−**5b** NPs/5-FU, and PLGA−TSPO−**6** NPs/5-FU) and dual drug loaded PLGA NPs/5-FU/**1** and PLGA−TSPO−**4a** NPs/5-FU/**1** were obtained by the DESD method (w/o/w).[35] Applying the first method the appropriate TSPO-ligands PLGA conjugate (**4a,b**, **5a,b**, and **6**) (30 mg) was dissolved in acetone (3 mL) at room temperature (ca. 25 °C) and poured into 30 mL of an aqueous solution of 0.1% (w/v) Lutrol F68. The resulting mixture was homogenized using a T25 Ultra-Turrax homogenizer (Janke and Kunkel, Germany) equipped with an S25N dispersing tool at 13 000 rpm for 30 s and then stirred for overnight to evaporate the organic solvent. The suspension was then transferred into Eppendorf vials and centrifuged at 13 200 rpm for 30 min (Eppendorf centrifuge, model 5415 D). The NPs thus obtained were washed with deionized water and then were finally resuspended in 1 mL of water and lyophilized for 24 h at −50 °C (ALPHA 1−4 LSC model, CHRIST freeze-drier, Osterode am Harz, Germany). For the encapsulation of free TSPO-ligand **1** into PLGA NPs (PLGA NPs/**1**), 30 mg of polymer (PLGA **3a**) and 5 mg of TSPO ligand **1** were codissolved in acetone and then used to prepare the desired NPs, following the same procedure. Blank PLGA NPs were prepared as controls following the above procedure.

PLGA−TSPO NPs loaded with 5-FU were prepared using a water−oil−water (w/o/w) emulsion solvent evaporation method. Briefly 5 mg/mL of 5-FU dissolved in phosphate buffer solution (50 mM, pH 7.4) was emulsified in 3 mL of acetone containing 0.5% (w/v) Lutrol F68 and the appropriate TSPO ligand−PLGA conjugate (30 mg) by Ultra-Turrax homogenizer at 13 000 rpm for 60 s. This w/o emulsion was added to 30 mL of phosphate buffer solution (50 mM, pH 7.4) containig 0.1% (w/v) of Lutrol F68 and emulsified using again an Ultra-Turrax (13 000 rpm for 60 s). The resultant w/o/w emulsion was agitated with a magnetic stirrer for 3 h at room temperature. The suspension was then transferred into Eppendorf vials and centrifuged at 13 200 rpm for 30 min. The NPs thus obtained were washed quickly with distilled water and finally resuspended in 1 mL of water and lyophilized for 24 h at −50 °C. 5-FU loaded PLGA NPs (PLGA NPs/5-FU) were prepared following the above procedure started with PLGA RG502H **3a**. For the encapsulation of free TSPO ligand **1** into dual drug loaded NPs (PLGA NPs/5-FU/**1** and PLGA−TSPO−**4a** NPs/5-FU/**1**), 30 mg of polymers (PLGA **3a** for PLGA NPs/5-FU/**1** and TSPO-ligand PLGA conjugate **4a** for TSPO−**4a** NPs/5-FU/**1**, respectively) and 5 mg of compound **1** were codissolved in acetone and then used to prepare the desired NPs, following the same procedure.

Fluorescent labeled FITC−PLGA−TSPO NPs and FITC−PLGA NPs were prepared using by QSESD technique following the same procedure described for PLGA−TSPO NPs. These formulations were stored at 4 °C until further use.

Physicochemical Characterization of NPs. The mean size and polydispersity index (PDI) of the NPs suspension were measured using a Zetasizer Nano ZS (Malvern Instruments Ltd., Worcestershire, UK) after suitable dilution of bulk suspensions in demineralized water. The zeta potential, that is, the surface charge of NPs, was determined by laser Doppler velocimetry with the same instrument after dilution with 1 mM KCl.

The morphological examination of NPs was performed by transmission electron microscopy (TEM) (CM12 Philips, Eindhoven, The Netherlands). Drops of water-resuspended NPs were stained with 2% (w/v) phosphotungstic acid and were placed on copper grids with Formvar films for TEM observation.

Determination of 5-FU and 1 Contents. The encapsulation efficiency (EE) of the NPs was defined as the percentage of 5-FU or **1** respectively encapsulated, in respect to the total amount of 5-FU or **1** used to prepare the NPs. The 5-FU or **1** loading was calculated as milligrams of 5-FU or **1** encapsulated relative to one gram of the lyophilized loaded NPs.

The amount of compounds included in the polymeric NPs was determined using a direct procedure. 5-FU-loaded NPs (2 mg) were dissolved in chloroform (1 mL), 5-FU was extracted in phosphate buffer (1 mM, pH 7.4),[30] and quantified by high-performance liquid chromatography (HPLC) method. Instead to quantify TSPO ligand **1** loaded in PLGA NPs/**1**, PLGA NPs/5-FU/**1** and PLGA−TSPO NPs/5-FU/**1**, NPs (2 mg) were dissolved in chloroform (1 mL), and the polymer was precipitated by diethyl ether (2.5 mL). The organic phase was then collected and dried under reduced pressure. The residue was dissolved in methanol (1 mL), and TSPO ligand **1** was quantified by the HPLC method.

***In Vitro* Release Studies.** *In vitro* release of drug from NPs formulation was studied in phosphate buffer (pH 7.4 in 0.05 M) at 37 °C. NPs suspensions (1 mg/mL) were prepared in buffer solution (pH 7.4 in 0.05 M) and maintained in a shaker water bath at the constant temperature of 37 ± 0.2 °C. Periodic samples (1 mL) were taken and replaced with fresh phosphate buffer of equivalent volume. Each sample was then centrifuged at 13 200 rpm for 10 min, and the supernatant was removed

dx.doi.org/10.1021/mp400536z | *Mol. Pharmaceutics* 2014, 11, 859−871

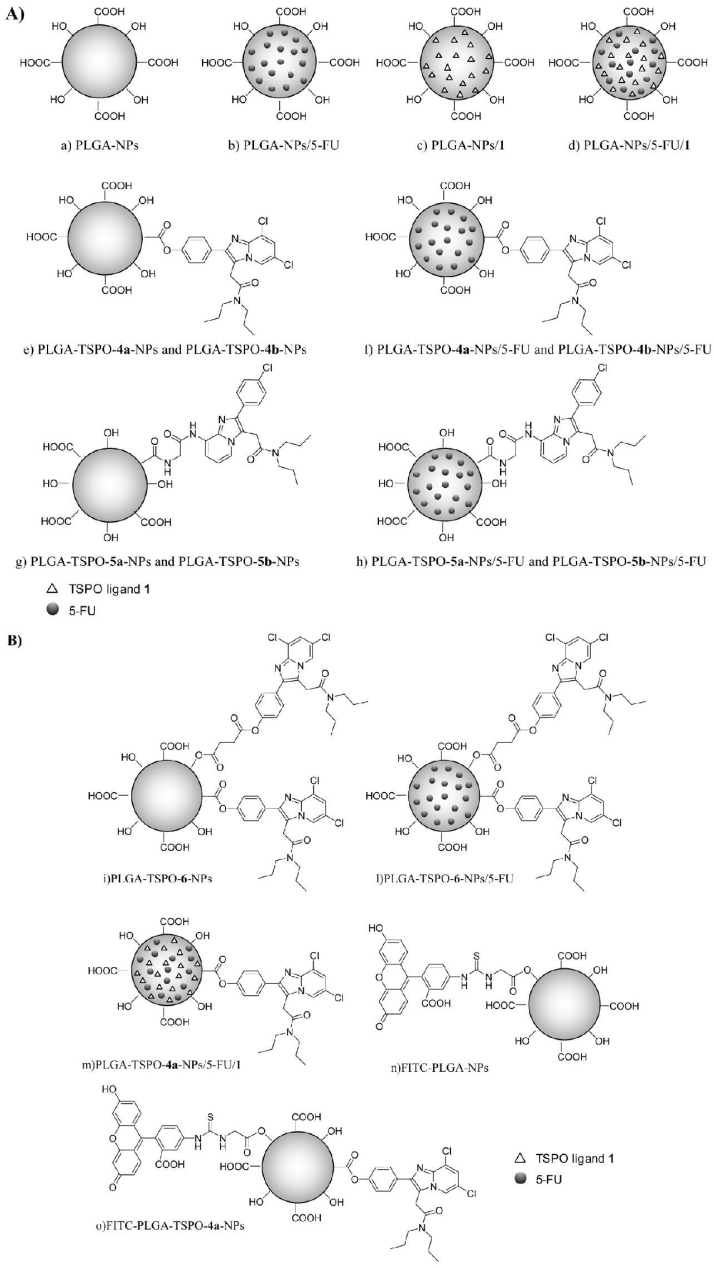

Figure 1. (A–B) Schematic representation of unloaded and loaded NPs based on PLGA or TSPO ligand–PLGA conjugates.The PLGA NPs (a–d) were prepared started on a PLGA that has a free hydroxyl and carboxylic acid group at its terminal ends. The PLGA carboxylic end group was conjugated to TSPO ligand **1** and **2**, to obtained TSPO ligand–PLGA conjugates **4**–**6**, which have been used as started polymers to build unloaded TSPO ligand **1** functionalized NPs (PLGA–TSPO–**4a** NPs, PLGA–TSPO–**4b** NPs, and PLGA–TSPO–**6** NPs) (e and i) and unloaded PLGA–TSPO ligand **2** functionalized NPs (PLGA–TSPO–**5a** NPs and PLGA–TSPO–**5b** NPs) (g), respectively. 5-FU loaded PLGA–TSPO NPs (f, h, and l) and dual drug loaded PLGA NPs (PLGA NPs/5FU/**1**) (d), and PLGA–TSPO NPs (PLGA–TSPO NPs/5FU/**1**) (m) were prepared by a double emulsion solvent diffusion method. Moreover the PLGA hydroxylic end group was conjugated to fluorescent probe FITC, in order to prepare fluorescent FITC–PLGA NPs (n) and FITC–PLGA–TSPO NPs (o).

and filtered through cellulose acetate membranes (0.22 μm, Advantec MFS, Pleasanton, CA, USA). Then 20 μL of filtrates was directly analyzed by HPLC. All the experiments were performed in triplicate. Quantification of 5-FU and TSPO ligands **1** was done by measuring the peak area in relation to standard solution of the 5-FU and the ligand **1** respectively, chromatographed under the same conditions. The cumulative amount of compound released over time was expressed as the

Table 1. Characteristics of NPs: 5-FU and 1 Loading Efficiency, Encapsulation Efficiency (EE), and Yield[a]

NPs set	NPs	polymer or stated conjugate	type of compound loaded	drug loading[b] (mg drug/g NP)	EE (%)	yield % (w/w)
	PLGA NPs	**3a**				85
	PLGA NPs/**1**	**3a**	**1**	110.0 ± 28	77.7 ± 15.5	88
	PLGA NPs/5-FU/**1**	**3a**	5-FU + **1**	17.5 ± 2.8 (5-FU)	10.7 ± 2.8 (5-FU)	58
				89.4 ± 10.0 (**1**)	48.1 ± 17.5 (**1**)	
	PLGA NPs/5-FU	**3a**	5-FU	43.9 ± 8.1	59.1 ± 2.0	76
PLGA–TSPO NPs	PLGA–TSPO–**4a** NPs	**4a**				85
	PLGA–TSPO–**4b** NPs	**4b**				54
	PLGA–TSPO–**6** NPs	**6**				69
	PLGA–TSPO–**5a** NPs	**5a**				80
	PLGA–TSPO–**5b** NPs	**5b**				80
	FITC–PLGA–TSPO NPs	**7**				52
	FITC–PLGA NPs	**8**				48
PLGA–TSPO NPs/5-FU	PLGA–TSPO–**4a** NPs/5-FU	**4a**	5-FU	42.5 ± 3.5	31.1 ± 12.0	62
	PLGA–TSPO–**4b** NPs/5-FU	**4b**	5-FU	36.6 ± 5.0	24.1 ± 0.9	60
	PLGA–TSPO–**6** NPs/5-FU	**6**	5-FU	15.8 ± 4.4	9.1 ± 1.1	57
	PLGA–TSPO–**5a** NPs/5-FU	**5a**	5-FU	28.5 ± 5.6	15.8 ± 4.2	64
	PLGA–TSPO–**5b** NPs/5-FU	**5b**	5-FU	29.7 ± 5.7	16.4 ± 3.5	89
	PLGA–TSPO NPs/5-FU/**1**	**4a**	5-FU + **1**	14.4 ± 2.8 (5-FU)	10.4 ± 1.8 (5-FU)	49
				71.0 ± 17.6 (**1**)	43.5 ± 10.2 (**1**)	

[a]Data are shown as media ± SD (n = 3). [b]Milligrams of compound **1** or 5-FU loaded for gram of NPs.

percent of the initial drug loaded in the NPs. Each data point is the mean ± standard deviation (S.D.) calculated on three measurements.

Differential Scanning Calorimetry (DSC) Analysis. DSC thermograms of 5-FU, TSPO ligand **1**, PLGA **3a**, TSPO-ligand PLGA conjugate **4a**, empty PLGA–TSPO NPs, and 5-FU loaded PLGA–TSPO NPs (PLGA–TSPO–**4a** NPs/5-FU and PLGA–TSPO–**4a** NPs/5-FU/**1**) were performed to analyze the physicochemical behavior of nanoparticles. DSC thermograms were obtained by a Mettler Toledo DSC 822 Star^e 2002 System equipped with a thermal analysis automatic program; indium was used as internal standard. Samples (about 5 mg) were placed in an aluminum pan and heated from 25 to 305 °C at a rate of 5 °C min^{-1} under a nitrogen flow of 50 cm^3 min^{-1}.

Cell Cultures. Rat C6 glioma cells were cultured in Ham's/F12 nutrient supplemented with 10% heat inactivated FBS, 2 mM L-glutamine, penicillin (100 U/mL), and streptomycin (100 μg/mL) (complete medium). Cells were maintained at 37 °C in a humidified atmosphere with 5% CO_2 and were fed every day. Cells were seeded in 96-well plates at a density of ∼5000 cells/well for viability assays, while for fluorescence microscopy cells were seeded in 6-well plates at a density of ∼100 000 cells/well. The following day, medium was changed with complete medium (untreated-cells) or with medium supplemented with the tested NPs at several concentrations of either 5-FU or the TSPO ligand **1**, and the cells were incubated for different times. The percentage of DMSO, the organic solvent in which the tested compounds 5-FU and **1** were dissolved, never exceeded 1% (v/v) in the samples. We verified that this amount did not affect cell viability.

Cell Viability Analysis by MTT Conversion and Combination Index (CI) Calculations. The number of living cells was assessed by a quantitative colorimetric tetrazolium salt reduction (MTT) assay. In particular, 200 μL of cell suspension were plated in 96-well plates at a density of ∼5000 cells/well. After 1 day of incubation at 37 °C in a humidified atmosphere with 5% CO_2, the culture medium was replaced with the same volume of fresh complete medium or with medium containing different concentrations of the tested compounds. Untreated cells were used as a positive control, and cells incubated with a 2% (w/v) sodium dodecyl sulfate (SDS) solution were used as a negative control. After the incubation period of 24 h, 10 μL of a 0.5% (w/v) MTT/PBS solution were added to each well, and the incubation was prolonged for further 4 h. After this period, medium was removed and replaced with 150 μL of a DMSO/ethanol (1:1) solution per well. The absorbance of the individual well was measured by microplate reader (Wallac Victor3, 1420 Multilabel Counter, Perkin-Elmer). Each drug concentration was tested in triplicate, and the experiments were repeated three times.

The cytotoxic effects measured for PLGA NPs/**1**, PLGA NPs/5-FU, PLGA NPs/5-FU/**1**, PLGA–TSPO–**4a** NPs, PLGA–TSPO–**4a** NPs/5-FU, and PLGA–TSPO–**4a** NPs/5-FU/**1** were further analyzed according to the Chou and Talalay method on CompuSyn software (ComboSyn, Inc., Paramus, NJ, USA).[36] The combination index (CI) was calculated according to the equation of Chou-Talalay for two drugs: $CI = (D)_1/(Dx)_1 + (D)_2/(Dx)_2$, where in the denominators, $(Dx)_1$ is the dose of $Drug_1$ alone that inhibits x%. Likewise, $(Dx)_2$ is the dose of $Drug_2$ alone that inhibits x%. In the numerators, $(D)_1$ is the portion of $Drug_1$ in combination $(D)_1 + (D)_2$ also inhibits x % and, again, likewise with $(D)_2$. PLGA NPs/5-FU/**1** and PLGA–TSPO–**4a** NPs/5-FU were considered at a fixed-dose-

Table 2. Hydrodynamic Diameter (Size), Polydispersity (PDI), and Zeta Potential (PZ) of NP Formulations[a]

NP set	NPs	size (nm)	PDI	PZ (mV)
	PLGA NPs	165.2 ± 28.7	0.21 ± 0.01	−34.6 ± 1.9
	PLGA NPs/**1**	133.0 ± 18.3	0.24 ± 0.07	−39.5 ± 2.7
	PLGA NPs/5-FU/**1**	150.0 ± 12.2	0.08 ± 0.01	−46.7 ± 2.3
	PLGA NPs/5-FU	117.8 ± 15.6	0.43 ± 0.03	−37.8 ± 2.4
PLGA−TSPO NPs	PLGA−TSPO−**4a** NPs	115.5 ± 10.1	0.09 ± 0.02	−37.6 ± 1.0
	PLGA−TSPO−**4b** NPs	122.9 ± 1.6	0.07 ± 0.01	−27.3 ± 3.2
	PLGA−TSPO−**6** NPs	170.4 ± 2.6	0.07 ± 0.02	−30.9 ± 2.8
	PLGA−TSPO−**5a** NPs	195.0 ± 0.9	0.12 ± 0.01	−29.2 ± 3.3
	PLGA−TSPO−**5b** NPs	81.1 ± 0.9	0.15 ± 0.01	−31.2 ± 2.7
	FITC−PLGA−TSPO NPs	84.8 ± 1.6	0.23 ± 0.03	−22.7 ± 1.3
	FITC−PLGA NPs	94.7 ± 0.7	0.18 ± 0.01	−31.2 ± 2.7
PLGA−TSPO NPs/5-FU	PLGA−TSPO−**4a** NPs/5-FU	165.0 ± 2.0	0.13 ± 0.01	−39.5 ± 2.7
	PLGA−TSPO−**4b** NPs/5-FU	168.4 ± 6.1	0.08 ± 0.02	−38.1 ± 2.4
	PLGA−TSPO−**6** NPs/5-FU	168.6 ± 4.3	0.15 ± 0.41	−33.4 ± 1.6
	PLGA−TSPO−**5a** NPs/5-FU	130.3 ± 1.7	0.15 ± 0.02	−51.9 ± 2.5
	PLGA−TSPO−**5b** NPs/5-FU	175.1 ± 3.2	0.11 ± 0.01	−37.5 ± 2.2
	PLGA−TSPO NPs/5-FU/**1**	147.6 ± 7.0	0.25 ± 0.08	−37.5 ± 2.2

[a]Data are shown as media ± SD (n = 3).

ratio combination of their building blocks: compound **1** and 5-FU (8:1 and 1.7:1, respectively). CI = 1 indicates an additive effect in the absence of synergism or antagonism; CI < 1 indicates synergism; CI > 1 indicates antagonism.

Fluorescence Microscopy. Fluorescence of cells was examined through an inverted Zeiss Axiovert 200 microscope (Zeiss, Milano, Italy) equipped with a 63 × 1.4 oil objective. The uptake of 0.2 μM fluorescent labeled NPs (FITC−TSPO NPs) into rat C6 glioma cells was imaged after the incubation for 4, 8, and 24 h at 37 °C in a 5% CO_2 atmosphere. Excitation and emission wavelengths of FITC-conjugated probe were selected with appropriate filters (Filter set Zeiss 10: excitation filter BP 450−490 nm; beamsplitter, dichroic mirror FT 510 nm; emission filter 540BP25 nm) mounted in Lambda 10-2 filter wheel controllers (Sutter Instruments, Novato, CA, USA), and fluorescence images were captured by a CoolSNAP HQ CCD camera (Roper Scientific, Trenton, NJ) using the Metamorph/Metafluor software (Universal Imaging Corporation). The average emission intensity of fluorescent cells was measured every 30 s for 5 min subtracting the background. During this period of time, the FITC emission intensities remained stable within ±5%. In each acquisition 20−30 cells were selected, and measurements were repeated 5 times using cells from independent cultures. All data are given as means ± SD.

Statistical Analysis. All data are presented as mean ± SD. The statistical analysis of cytotoxicity was accomplished using one-way analysis of variance (ANOVA) followed by the Bonferroni post hoc tests (GraphPad Prism version 4 for Windows, GraphPad Software, San Diego, CA). Differences were considered statistically significant at $p < 0.05$. For calculation of EC_{50} values, the nonlinear multipurpose curve-fitting program SigmaPlot 9.0 was used.

In fluorescence microscopy studies the data are given as means ± SD (bars) for five separate cultures. The statistical significance of differences was calculated by the unpaired Student's t test with Bonferroni's correction. *$P < 0.05$, **$P < 0.005$.

RESULTS

Preparation and Characterization of NPs. All of the prepared NPs are shown in Figure 1A−B. The yield, the drug encapsulation, and the loading efficiency are listed in Table 1. Sizes, size distributions, and the zeta potential of the NPs were characterized using a Zetasizer Nano ZS instrument, and the results were reported in Table 2 and in Figure 2. The PLGA−TSPO NPs set includes the following formulations: PLGA−TSPO−**4a** NPs (Figure 1A, e), PLGA−TSPO−**4b** NPs (Figure 1A, e), PLGA−TSPO−**5a** NPs (Figure 1A, g), PLGA−TSPO−**5b** NPs (Figure 1A, g), and PLGA−TSPO−**6** NPs (Figure 1B, i). PLGA−TSPO NPs were prepared by QESD methods with a good yield, started from five different TSPO ligand−PLGA conjugates **4a**,**b**, **5a**,**b**, and **6**, respectively. PLGA−TSPO NPs set exhibit diameters between 81 and 195 nm and a low polydispersity index (PDI). Analysis of the zeta potential of PLGA−TSPO NPs suspended in 1 mM KCl demonstrates that all PLGA−TSPO-NPs were characterized by negative surface charges that ranged from −29.2 to −37.6 mV. The process yield was calculated as amount of lyophilized NPs relative to the amount of solid materials used in the process. PLGA NPs/**1** (Figure 1A, c) were also prepared by QESD methods with a good yield, started from PLGA polymer **3a**, and showed a high EE of 77.7% with a loading efficiency of 110.0 mg/g. PLGA NPs/**1** showed an average hydrodynamic diameter of 133.0 nm with a high negatively charged surface of −39.5 mV.

PLGA NPs/5-FU (Figure 1A, b) and the five formulations of PLGA−TSPO-NPs/5-FU set, that is, PLGA−TSPO−**4a** NPs/5-FU (Figure 1A, f), PLGA−TSPO−**4b** NPs/5-FU (Figure 1A, f), PLGA−TSPO−**5a** NPs/5-FU (Figure 1A, h), PLGA−TSPO−**5b** NPs/5-FU (Figure 1A, h), and PLGA−TSPO−**6** NPs/5-FU (Figure 1B, l) were prepared by DESD methods with a discrete yield, started from PLGA **3a** and with TSPO ligand−PLGA conjugates **4a**,**b**, **5a**,**b**, and **6**, respectively. The hydrodynamic diameters of TSPO-NPs/5-FU ranged from 130.3 to 175.1 nm, and they have a negative surface charge with an average value between −33.4 and −51.9 mV. The PLGA−TSPO-NPs/5-FU had a low EE between 9.1 and 31.1%, with a discrete 5-FU loading efficiencies, instead PLGA NPs/5-FU have higher EE of 59.1% with a loading efficiency of 43.9 mg/g. In particular TSPO−**4a** NPs showed an average hydrodynamic

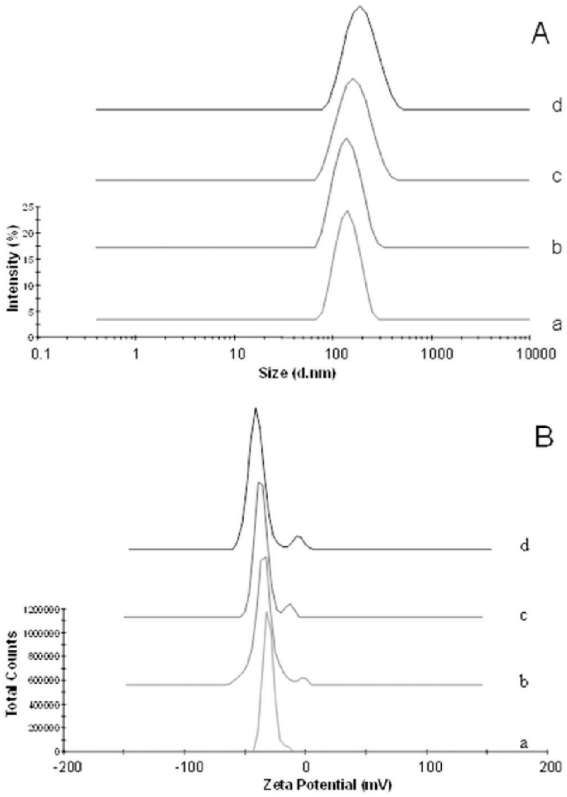

Figure 2. Particle size distribution (A) and zeta distribution (B) of PLGA–TSPO–**4a** NPs (a), PLGA NPs/5-FU (b); PLGA–TSPO–**4a** NPs/5-FU/**1** (c) and PLGA–TSPO–**4a** NPs/5-FU (d).

diameter near 100 nm (115.5 ± 10.1 nm), as also confirmed by the average diameter obtained by TEM analysis, a very low polydispersity (0.09 ± 0.02), with a high negatively charged surface of −37.6 mV (Figure 2). Moreover, PLGA–TSPO–**4a** NPs/5-FU showed the highest 5-FU loading efficiency and EE of 42.5 mg/g and 31.1%, respectively. PLGA–TSPO–**4b** NPs and PLGA–TSPO–**4b** NPs/5-FU show similar features of the formulations above prepared starting from polymer **4a** but have a low percentage of TSPO ligand **1** covalently linked to the polymeric carrier.[25] On the other hand, PLGA–TSPO–**5b** NPs had an suitable average diameter of 81.1 ± 0.9 nm, which increase in size to 175.1 ± 3.2 nm when 5-FU is loaded. In fact, the resulting PLGA–TSPO–**5b** NPs/5-FU are characterized by a 5-FU loading efficiency and EE of 29.7 mg/g and 16.4%, respectively. Furthermore, a low conjugation degree of TSPO ligand **2** linked to PLGA polymer conjugate **5b** was observed.[25] PLGA–TSPO–**6** NPs, which have the highest conjugation degree of TSPO ligand **1**, shown to load the lower amount of 5-FU most likely due to the high hydrophobic nature of the started polymer **6**, as confirmed by the its high PZ value of −33.4 mV (Table 2). Dual drug loaded PLGA NPs/5-FU/**1**, (Figure 1A, d), and PLGA–TSPO–**4a** NPs/5-FU/**1** (Figure 1B, m), had average diameters of 150.0 nm and 147.6 nm, respectively, and a negative charge of −46.7 (PLGA NPs/5-FU/**1**) and −37.5 mV (PLGA–TSPO NPs/5-FU/**1**). The EE % were 10.7% (5-FU) and 48.1% (TSPO ligand **1**) for PLGA NPs/5-FU/**1** and 10.4% (5-FU) and 43.5% (TSPO ligand **1**) for PLGA–TSPO NPs/5-FU/**1**.

TEM micrograph of TSPO–**5a** NPs, TSPO–**4a** NPs/5-FU, FITC–TSPO NPs, PLGA NPs/5-FU/**1**, and TSPO NPs/5-FU/**1** are shown in Figure 3. In particular, TEM analysis

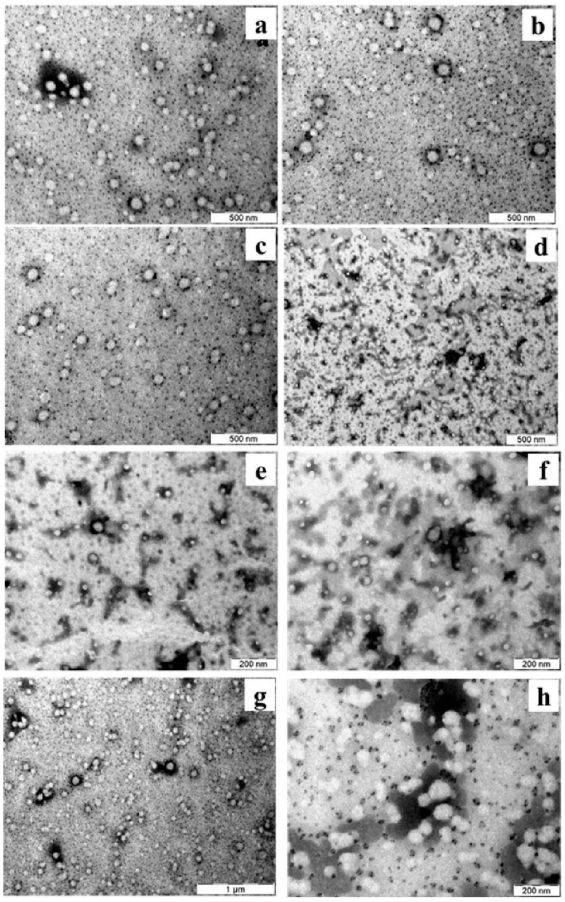

Figure 3. Transmission electron micrographs of NPs: PLGA–TSPO–**4a** NPs (a); PLGA–TSPO–**5a** NPs (b); PLGA–TSPO–**4a** NPs/5-FU (c); FITC–PLGA–TSPO NPs (d–e); PLGA NPs/5-FU/**1** (f) and PLGA–TSPO NPs/5-FU/**1** (g–h).

showed that TSPO–PLGA NPs and TSPO–PLGA NPs/5-FU are well-dispersed and have diameters smaller than the ones measured by dynamic light scattering. Most of these nanoparticles are characterized by a spherical shape, and the presence of some extended shapes, evidenced for FITC-TSPO-NPs, is due to the presence of aggregates. However, these aggregation properties are more evident for TSPO-NPs/5-FU/1 than FITC-TSPO-NPs (Figure 3, panel h and d, respectively). DLS and TEM analysis confirm the colloidal stability of dispersed particles.

DSC thermograms of free 5-FU, TSPO ligand **1**, PLGA **3**, TSPO ligand PLGA conjugate **4a**, 5-FU and PLGA physical mixture, empty NPs, 5-FU-loaded TSPO NPs (TSPO–**4a** NPs/5-FU) are shown in Figure 4. The curves of 5-FU and TSPO-ligand **1** are characterized by the presence of endothermic peaks of pure compounds at 286.9 °C and at

dx.doi.org/10.1021/mp400536z | *Mol. Pharmaceutics* 2014, 11, 859–871

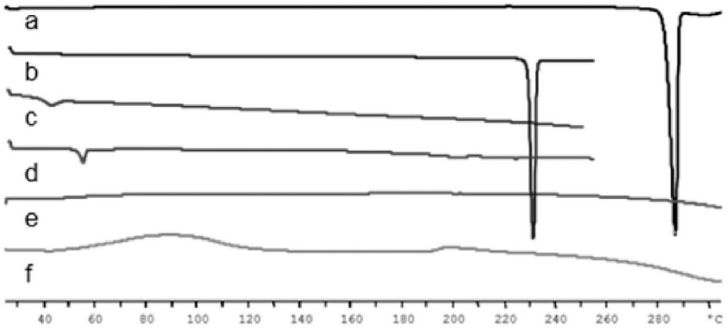

Figure 4. DSC thermograms of 5-FU (a), TSPO ligand **1** (b), PLGA **3a** (c), TSPO ligand PLGA conjugate **4a** (d), PLGA−TSPO−**4a** NPs (e), and PLGA−TSPO−**4a** NPs/5-FU) (f).

226 °C, respectively. NPs formulations evaluated are amorphous, and PLGA and **4a** polymers show evident glass transition temperature (T_g) peaks around 50 °C.

***In Vitro* Drug Release.** The in vitro release profile of 5-FU loaded NPs was investigated in PBS at 37 °C. The cumulative percentage release of 5-FU from PLGA NPs/5-FU, TSPO−**4a** NPs/5-FU, PLGA NPs/5-FU/**1**, and TSPO NPs/5-FU/**1** are shown in Figure 5a,b. All 5-FU loaded NPs showed a biphasic release profiles with an initial common burst release in the first 1 h followed by a slower phase with a sustained release of 5-FU from NPs over 72 h. PLGA NPs/5-FU/**1** in the first hour showed the highest drug release that was equivalent to 53.0 ± 14.7% of the initial drug load. The amount of cumulated 5-FU release from TSPO NPs/5-FU/**1**, PLGA NPs/5-FU/**1**, TSPO−**4a** NPs/5-FU, and PLGA NPs/5-FU, after 24 h, was 90.4 ± 4.8%, 85.6 ± 3.7%, 75.8 ± 5%, and 65.7 ± 16.1%, respectively. While the total amount of drug (expressed as milligrams of drug released per gram of NPs) was equal to 32.2 ± 3.7% mg/g for TSPO−**4a** NPs/5-FU, 28.8 ± 7.5% mg/g for PLGA NPs/5-FU, 15.0 ± 3.4% for PLGA NPs/5-FU/**1**, and 13.0 ± 3.6% for TSPO NPs/5-FU/**1**. PLGA NPs/**1**, PLGA NPs/5-FU/**1**, and TSPO NPs/5-FU/**1** were also assessed in PBS at 37 °C to determine the release profile of the TSPO ligand **1** incorporated, and the relative release profiles were shown in Figure 5c,d. Dual drug loaded NPs showed an initial burst release phase with about 10−15% of the ligand released in the first 1 h followed by a sustained release over 72 h that may be due to diffusion from the polymeric matrix. After 24 h the total amount of cumulated ligand released from PLGA NPs/**1**, PLGA NPs/5-FU/**1**, and TSPO NPs/5-FU/**1** was 17.9 ± 1.9%, 29.2 ± 8.1%, and 25.8 ± 9.0%, respectively, and after 120 h became 31.3 ± 6.0% for PLGA NPs/**1**, 35.7 ± 7.2 for PLGA NPs/5-FU/**1**, and 36.2 ± 2.4 for TSPO NPs/5-FU/**1**, while the total amount of compound was equivalent to 28.4 ± 5.5 mg/mL for PLGA NPs/**1**, 31.9 ± 5.0 for PLGA NPs/5-FU/**1**, and 25.7 ± 9.0 for TSPO-NPs/5-FU/**1**.

Induction of Cell Death. *In vitro* cytotoxicity of free 5-FU and TSPO ligand **1**, unloaded PLGA NPs (PLGA NPs) PLGA NPs/**1**, and selected 5-FU loaded PLGA NPs: PLGA NPs/5-FU, TSPO−**4a** NPs/FU, and TSPO NPs/5-FU/**1** was evaluated using the MTT assay. In particular, we investigated the ability of the above-mentioned compounds and nanovectors to interfere with the cell survival of rat C6 glioma cells. This tumor cell line was chosen because it is well-known that the TSPO protein is highly expressed on glial tumors.[37] Cell viability was determined quantitatively by the MTT conversion assay. In Table 3 are reported the IC_{50} values (i.e., the concentration inducing 50% cell survival inhibition) obtained from dose response curves. Blank PLGA NPs used as a control at a concentration of 1 mg/mL showed no toxicity, while free anticancer drug and TSPO ligand **1** exhibited an IC_{50} value of 1.46 ± 0.06 and 17.5 ± 0.7, μM, respectively. In Table 3 the IC_{50} values were entered as absolute values and as values normalized to take into account the relative drug loading of 5-FU or TSPO ligand.

The rank order of IC_{50} values (concentrations referred to 5-FU) for formulations of 5-FU loaded NPs were 27.17 ± 1.07 (PLGA NPs/5-FU), 1.83 ± 0.03 (TSPO-NPs/5-FU/**1**), 1.07 ± 0.04 (PLGA NPs/5-FU/**1**) and 0.88 ± 0.07 (TSPO−**4a** NPs/5-FU), μM, respectively. However, for the TSPO-ligand **1** the ranking order of IC_{50} values becomes: 209.0 ± 0.1 (PLGA-NPs/**1**), 23.95 ± 0.96 (TSPO−**4a** NPs), 18.5 ± 0.74 (TSPO-NPs/5-FU/**1**), 3.02 ± 0.12 (PLGA NPs/5-FU/**1**) and 1.94 ± 0.08 (TSPO−**4a** NPs/5-FU), μM, respectively. While considering the values normalized on the basis of drug loading (relative value) the rank order of IC_{50} values (concentrations referred to 5-FU) for 5-FU loaded NPs becomes: 0.13 (PLGA−TSPO−**4a** NPs/5-FU/1), 0.21(PLGA−TSPO−**4a** NPs/5-FU), 0.61(PLGA NPs/5-FU/1), and 0.62(PLGA NPs/5-FU), μM, respectively. However, for the TSPO-ligand 1 the ranking order of IC_{50} values becomes: 0.26 (PLGA−TSPO−**4a** NPs/5-FU/1), 0.34 (PLGA NPs/5-FU/1), 1.90 (PLGA NPs/1), and 1.94 (PLGA−TSPO−**4a** NPs/5-FU) μM, respectively.

Uptake Studies of FITC−TSPO Nanoparticles (FITC−TSPO NPs) into Rat C6 Glioma Cells. The internalization of FITC−PLGA−TSPO NPs into rat C6 glioma cells, was investigated by fluorescence microscopy. The integrity of control cells was confirmed incubating the cells with specific markers which highlight the healthy of the selected organelle. In particular, in the present study we have imaged the mitochondrial network incubating cells with 25 nM Mito-Tracker Red CMXRos, thus highlighting the morphology of healthy mitochondrial network in control C6 glioma cells (Figure 6, panel iv). As shown in Figure 6 (panels i−iii,vi), cells treated with 0.2 μM of FITC−PLGA−TSPO NPs (concentration is referred to FITC), revealed a time-dependent increase of internalized green fluorescence that widely diffused in the cytosol of the cells. By contrast, no green fluorescence was imaged when cells were incubated in the presence of FITC (7 μM) (panel v), thus demonstrating that the internalized fluorescence of the cells was exclusively due to the cellular

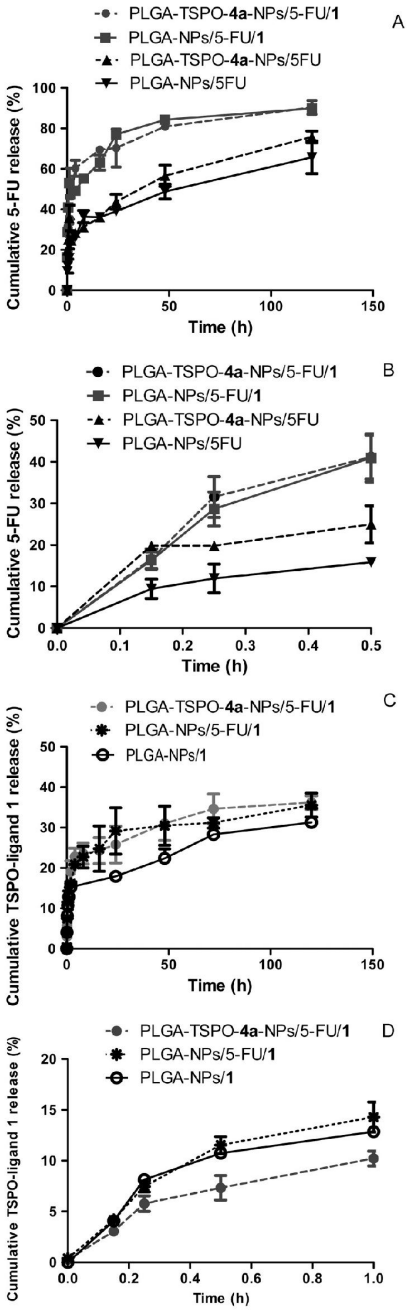

Figure 5. *In vitro* release profiles of 5-FU from PLGA–TSPO–**4a** NPs/5-FU/**1**, PLGA NPs/5-FU/**1**, PLGA–TSPO–**4a** NPs/5-FU, and PLGA NPs/5-FU in phosphate buffer at 37 °C and pH 7.4 after 120 h (a) and in first half hour (b). *In vitro* release profiles of TSPO-ligand **1** from PLGA NPs/5-FU/**1** and PLGA–TSPO–**4a** NPs/5-FU/**1** in phosphate buffer at 37 °C and pH 7.4 after 120 h (c) and in first hour (d). Values were reported as averages and standard deviations (mean ± SD, n = 3).

uptake of FITC-conjugated probe. In addition, by comparing uptake studies conducted with FITC–TSPO NPs, FITC NPs, or FITC–TSPO NPs in combination with TSPO ligand **1**, no significant differences were observed (data not shown), proving that, as expected, the TSPO moiety does not influence the uptake of the NPs inside cells. Since TSPO is a subcellular target, once ligands are delivered inside the cells they can bind the mitochondrial protein inducing apoptosis.

Table 3. IC_{50} Values of Free 5-FU, TSPO Ligand 1, and the NPs after 72 h Incubation with C6 Glioma Cancer Cell

NPs[a]	IC_{50} (μM), concentration referred to 5-FU	relative value[c]	IC_{50} (μM), concentration referred to TSPO ligand **1**	relative value[c]
5-FU	1.46 ± 0.06	1.46		
1			17.5 ± 0.70	17.5
PLGA NPs	>1[b]	>1[b]	>1[b]	>1[b]
PLGA NPs/**1**			209.0 ± 0.10	1.9
PLGA NPs/5-FU/**1**	1.07 ± 0.04	0.61	3.02 ± 0.12	0.34
PLGA NPs/5-FU	27.17 ± 1.07	0.62		
PLGA–TSPO–**4a** NPs			23.95 ± 0.96	23.95
PLGA–TSPO–**4a** NPs/5-FU	0.88 ± 0.03	0.21	1.94 ± 0.08	1.94
PLGA–TSPO–**4a** NPs/5-FU/**1**	1.83 ± 0.07	0.13	18.5 ± 0.74	0.26

[a]Data are shown as media ± SD (n = 3). [b]The concentration referrs to mg of PLGA per mL of suspension. [c]Values were normalized on the basis of drug loading.

DISCUSSION

In a previous report of our work, we investigated TSPO ligand–PLGA macromolecular conjugates characterized by high affinity and selectivity toward the 18 kDa mitochondrial translocator protein. Results suggested that in addition to modulating neurosteroid synthesis, they could be considered as macromolecular apoptosis inducing agents and, hence, able to induce tumor cell death. In fact, *in vitro* cytotoxicity studies outlined the ability of these TSPO polymer conjugates to constrain C6 glioma cells survival with EC_{50} values (i.e., the concentration inducing 50% cell survival inhibition) ranging from 1.75 to 34.29 μM and, moreover, to induce mitochondrial morphology modifications.[25] As a consequence, the obvious subsequent step of our research was focused on the formulation of these TSPO ligand–PLGA conjugates into nanoparticulate anticancer drug delivery system loaded with 5-FU, chosen as a model of hydrophilic anticancer drug, to obtain NPs potentially useful for anticancer therapy. Dual drug loaded NPs, with 5-FU and TSPO ligand **1**, were successfully achieved. Dual drug loaded PLGA–TSPO–**4a** NPs/5-FU/**1** have the advantage of delivering the TSPO ligand **1** through a chemical conjugation as well as by physical encapsulation.

Although the double emulsion (w/o/w) technique is used to incorporate hydrophilic drugs into micro- and nanoparticles prepared starting from hydrophobic polymers,[38] the low EE of 5-FU into 5-FU loaded NPs is probably mainly due to the hydrophilic nature of drug, the drug concentration in the internal aqueous phase and the PLGA concentration in the organic phase.[31,39] Moreover, the different EE % values can be attributed to the characteristics of the several polymers used in NP formulations. In fact, PLGA lipophilic/hydrophilic properties change after conjugations with TSPO ligands. After encapsulation of 5-FU in PLGA–TSPO–**4a** NPs and PLGA–TSPO–**4b** NPs, the size increased significantly from 115.5 to 165.0 nm for PLGA–TSPO–**4a** NPs and from 122.9

dx.doi.org/10.1021/mp400536z | *Mol. Pharmaceutics* 2014, 11, 859–871

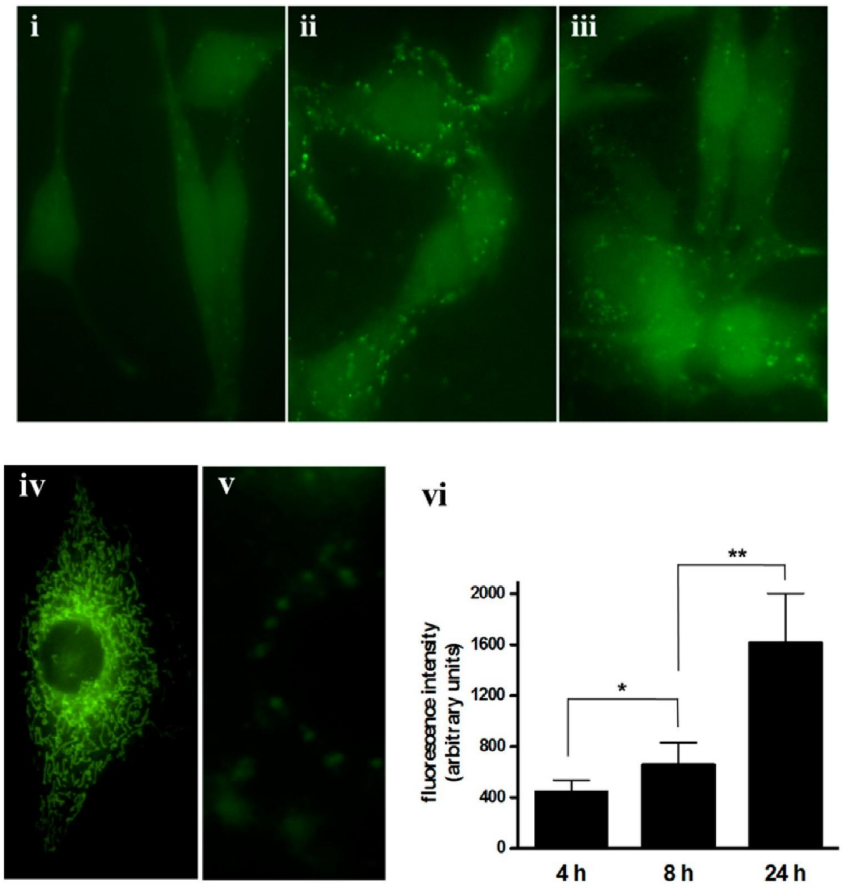

Figure 6. Cells were seeded onto 24 mm coverslips and treated at 37 °C in a 5% CO_2 atmosphere with 0.2 μM FITC−TSPO NPs (concentration is referred to FITC). Internalized FITC fluorescence was acquired after 4 (i), 8 (ii), and 24 h (iii). Images are representative of 4−6 independent experiments, and identical fields are presented. Cells incubated with 25 nM MitoTracker Red CMXRos (iv) and cells treatment with FITC (7 μM) alone after 24 h (v) were used as the control. Average intensity of internalized fluorescence of treated cells as imaged after 4, 8, and 24 h of incubation (vi). Data are given as means ± SD (bars) for five separate cultures. The statistical significance of differences was calculated by the unpaired Student's *t* test with Bonferroni's correction. *P < 0.05, **P < 0.005.

to 168.4 nm for PLGA−TSPO−**4b** NPs due to the high degree of encapsulation, compared to other drug loaded NPs. In fact in most nanoparticles the embedding of the 5-FU in NPs causes slightly increased size, with the exception of the PLGA−TSPO−**5b** NPs/5-FU. In the latter case the size reduction is probably due to the degradation of the polymer after the preparation of nanoparticles. In fact, the polymer becomes more hydrophilic, as shown by the increase in the zeta potential of NPs (from −29.2 to −51.9 mV). PLGA NPs/**1**, PLGA−TSPO−**4a** NPs, PLGA−TSPO−**4a** NPs/5-FU, and PLGA NPs/5-FU/**1** showed no aggregation in TEM images, which is attributed to the negative surface charges of the NPs and to the presence of some unconjugated hydroxyl and carboxylic acid groups at PLGA terminal ends, most likely expressed on the surface of the NPs. The morphology of 5-FU and TSPO ligand **1** loaded NPs revealed similar structures. FITC−TSPO NPs and PLGA−TSPO−**4a** NPs/5-FU/**1** showed the presence of some aggregates as confirmed by the PDI of 0.23 ± 0.03 and 0.25 ± 0.08, respectively.

Since TSPO ligand PLGA **4a** conjugate induce a mitochondrial morphology modification and for all the reasons described above (see the Results section), PLGA−TSPO−**4a** NPs, PLGA−TSPO−**4a** NPs/5-FU, and PLGA−TSPO−**4a** NPs/5-FU/**1** were chosen as reference formulations in the following studies. In particular, DSC, drug release, and *in vitro* cytotoxicity and uptake studies on C6 glioma cells were carried out. Thermal behavior studies showed that the physical mixtures, PLGA−TSPO−**4a** NPs/5-FU/**1** and PLGA−TSPO−**4a** NPs/5-FU do not exhibit the endothermic crystalline melting peaks of the pure compounds suggesting that 5-FU and TSPO ligand **1** are both dispersed in molecular form inside the polymer matrix as also confirmed by X-ray diffractogram of 5-FU loaded PLGA 50:50 NPs prepared by DESD (w/o/w) and reported elsewhere.[40]

Regarding the release studies, it should be highlighted that in PLGA-based nanoparticulate system, the polyester PLGA undergoes both bulk and surface erosion, as reported by Dinarvand et al.[41] Several already published works describe the initial burst release of 5-FU as the result of the dissolution of the drug located on the surface along with the surface erosion of the polymer matrix. Instead, the slow diffusion of the loaded drug in the core of the NPs, in combination with the polymeric

matrix degradation, causes a slow and sustained release of 5-FU. PLGA NPs/5-FU and PLGA−TSPO−**4a** NPs/5-FU exhibited significant differences regarding to cumulative percentage released of 5-FU after 72 h, compared to dual drug loaded PLGA NPs/5-FU/**1** and PLGA−TSPO−**4a** NPs/5-FU/**1** formulations. In fact, the rate of release from dual drug NPs appears to be greater although they have a lower drug loading. Regarding the *in vitro* release profiles of TSPO-ligand 1 from NPs is obvious that the ligand is released from the nanoparticles more slowly than 5-FU. The variation of release rate of the ligand is due to the slower diffusion of the hydrophobic ligand in the hydrophobic polymer matrix of PLGA. PLGA NPs/5-FU/**1** and PLGA−TSPO−**4a** NPs/5-FU/1 display no significant differences regarding to cumulative percentage released of TSPO-ligand after 120 h.

The *in vitro* cytotoxicity assay demonstrated that PLGA−TSPO-NPs/5-FU induce survival inhibition in rat C6 glioma cell line and uptake studies offered evidence that FITC-PLGA−TSPO-NPs penetrated into glioma cells. In the *in vitro* cytotoxicity studies were evaluated some NPs selected on the basis of the highest efficiency of embedding of 5-FU. Moreover were also included dual drug loaded PLGA NPs/5-FU/1 and PLGA−TSPO−**4a** NPs/5-FU/1 to highlight the occurrence of synergistic effects while unloaded PLGA NPs were used as reference. The results obtained shown that 5-FU loaded PLGA−TSPO NPs (PLGA−TSPO−**4a** NPs/5-FU, PLGA−TSPO−**4a** NPs/5-FU/**1**, and PLGA NPs/5-FU/**1**) are more cytotoxic that the PLGA NPs/5-FU, and furthermore PLGA−TSPO−**4a** NPs/5-FU showed the highest cytotoxicity compared with free 5-FU as well as the concentrations are related to TSPO ligand **1**, although dual drug loaded PLGA−TSPO NPs/5-FU/**1** do not appear to be more cytotoxic of the PLGA−TSPO NPs/5-FU. However, we have also considered that these nanoparticle systems have a different drug loaded. In fact, when the concentration is normalized (relative values), considering the correct load of 5-FU or TSPO ligand, the values show that PLGA NPs/5-FU/1, PLGA−TSPO−**4a** PLGA NPs/5-FU, and PLGA−TSPO−**4a** PLGA NPs/5-FU/1 are more cytotoxicity than 5-FU. Moreover the dual drug loaded PLGA−TSPO−**4a** NPs/5-FU/1 are more efficient of PLGA−TSPO−**4a** NPs/5FU both when the concentration is referred to 5-FU that when the concentration is referred to TSPO-ligand 1.

We have also evaluated the combination index (CI) which allows to compare the single-drug dose−response to that of their combination. In PLGA NPs/5-FU/**1** and PLGA−TSPO−**4a** NPs/5-FU the ratio between the TSPO ligand **1** and the anticancer drug 5-FU was set to 8:1 and 1.7:1, respectively. As presented in Table 4, in our experiments we have found that compound **1** was synergistic to 5-FU for both PLGA NPs/5-FU/**1** and PLGA−TSPO−**4a** NPs/5-FU on C6 cells at concentration of drugs leading to 50 and 75% cell survival. These results indicate that the assembling of the two building blocks, that is, the TSPO ligand **1** and 5-FU, produces NPs (PLGA NPs/5-FU/**1** and PLGA−TSPO−**4a** NPs/5-FU) pharmacologically profitable. Typical examples of CI/fractional effect (FA) curves are illustrated in Figure 7. These findings indicate that the apoptotic agent synergistically potentiates the antitumor effect of the anticancer drug 5-FU in rat C6 glioma cell line.

Table 4. CI Results in C6 Cells Corresponding to Concentration of Drugs Leading to 50 and 75% Cell Survival

	C6 cells	
NPs	50% CI[a]	75% CI[a]
PLGA NPs/5-FU/1	0.29	0.82
PLGA−TSPO−**4a** NPs/5-FU	0.25	0.37

[a]Combination index (CI) was calculated according to the equation of Chou-Talalay for two drugs on CompuSyn software (ComboSyn, Inc., Paramus, NJ. USA): CI = $(D)_1/(Dx)_1 + (D)_2/(Dx)_2$, where in the denominators, $(Dx)_1$ is the dose of $Drug_1$ alone that inhibits *x*%. Likewise, $(Dx)_2$ is the dose of $Drug_2$ alone that inhibits *x*%. In the numerators, $(D)_1$ is the portion of $Drug_1$ in combination $(D)_1 + (D)_2$ also inhibits *x*%. Again, likewise $(D)_2$. CI = 1 indicates additive effect in the absence of synergism or antagonism; CI < 1 indicates synergism; CI > 1 indicates antagonism.

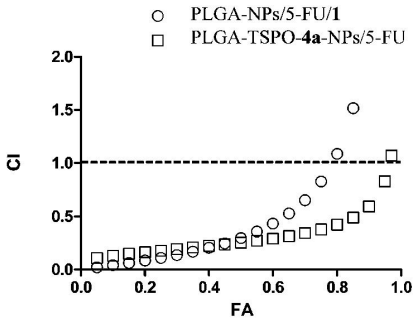

Figure 7. Typical examples of CI/fractional effects (FA) curves for C6 cells.

■ CONCLUSION

In conclusion the results achieved demonstrate that PLGA−TSPO NPs are potential carriers for selective delivery of anticancer drug in tumor cells overexpressing the TSPO and that the assembling of the two building blocks, that is, the TSPO ligand **1** and 5-FU, produces nanoparticles pharmacologically profitable. In fact, the dual drug loaded NPs (PLGA NPs/5-FU/**1**) and PLGA−TSPO NPs/5-FU (PLGA−TSPO−**4a** NPs/5-FU) could significantly enhance toxicity against human cancer cells due to the synergistic effect of the TSPO-ligand with anticancer drugs loaded in these systems.

The blood−brain barrier (BBB) limits access of NPs with large average diameter to the brain, even the BBB becomes impaired due to development of glioma. In literature it is documented that nanoparticles with mean diameters less than 200 nm might be able to permeate the BBB. Nevertheless, the further growth of the brain tumor, when both BBB and blood−brain tumor barrier (BBTB) become compromised, endothelial gaps form on the microvessels of brain tumors and enhanced permeability and retention (EPR) effect goes into action. Thus, in brain tumors and NPs can be addressed tumor tissue via passive targeting across BBB and BBTB, allowing NPs slightly larger to accumulate in tumor tissue much more than they do in normal tissues.[42,43] For these purposes the preparation of suitable injectable formulations of dual drug loaded NPs (PLGA−TSPO NPs/5-FU and PLGA−TSPO−**4a** NPs/5-FU) with the particle size and *in vivo* stability of NPs should be strictly controlled. Finally, drug delivery systems capable to release an anticancer drug together with a pro-apoptotic agent might have an enormous potential in anticancer therapy.

dx.doi.org/10.1021/mp400536z | *Mol. Pharmaceutics* 2014, 11, 859−871

Therefore, further *in vivo* studies are needed to prove the synergistic effect and the potential application of these dual drug loaded NPs.

■ AUTHOR INFORMATION

Corresponding Authors

*Phone/fax: +39 080 544 2767. E-mail: valentino.laquintana@uniba.it (V.L.).

*E-mail: nunzio.denora@uniba.it (N.D.).

Author Contributions

V.L. and N.D. contributed equally.

Notes

The authors declare no competing financial interest.

■ ACKNOWLEDGMENTS

This work was supported by a grant from Ministero dell'Università e della Ricerca (NANO Molecular tEcnologies for Drug delivery-NANOMED, PRIN 2010-2011 MIUR). The authors wish to acknowledgement ACRAF for their financial support. The sponsors played no role in the design, collection, or interpretation of the data, or writing of the manuscript. The authors would also like to thank Mr. Antonio Palermo and Mr. Giovanni Dipinto for their technical support and professional skills.

■ REFERENCES

(1) Papadopoulos, V.; Baraldi, M.; Guilarte, T. R.; Knudsen, T. B.; Lacapère, J. J.; Lindemann, P.; Norenberg, M. D.; Nutt, D.; Weizman, A.; Zhang, M. R.; Gavish, M. Translocator protein (18 kDa): new nomenclature for the peripheral-type benzodiazepine receptor based on its structure and molecular function. *Trends Pharmacol. Sci.* **2006**, *27*, 402−409.

(2) Veenman, L.; Gavish, M. Peripheral-type benzodiazepine receptors: their implication in brain disease. *Drug Dev. Res.* **2000**, *50*, 355−370.

(3) Galiegue, S.; Tinel, N.; Casellas, P. The peripheral benzodiazepine receptors: a promising therapeutic drug target. *Curr. Med. Chem.* **2003**, *10*, 1563−1572.

(4) Anholt, R. R. H.; Pedersen, P. L.; De Souza, E. B.; Snyder, S. H. The peripheral benzodiazepine receptor: localization to the mitochondrial outer membrane. *J. Biol. Chem.* **1986**, *261*, 576−583.

(5) Veenman, L.; Papadopoulos, V.; Gavish, M. Channel-like functions of the 18-kDa translocator protein (TSPO): regulation of apoptosis and steroidogenesis as part of the host-defense response. *Curr. Pharm. Des.* **2007**, *13*, 2385−2405.

(6) Veenman, L.; Gavish, M. The role of 18 kDa mitochondrial translocator protein (TSPO) in programmed cell death, and effects of steroids on TSPO expression. *Curr. Mol. Med.* **2012**, *12*, 398−412.

(7) Gatliff, J.; Campanella, M. The 18 kDa translocator protein (TSPO): a new perspective in mitochondrial biology. *Curr. Mol. Med.* **2012**, *12*, 356−368.

(8) Han, Z.; Slack, R. S.; Li, W.; Papadopoulos, V. Expression of peripheral benzodiazepine receptor (PBR) in human tumors: relationship to breast, colorectal, and prostate tumor progression. *J. Recept. Signal Transduct. Res.* **2003**, *23*, 225−238.

(9) Galiegue, S.; Casellas, P.; Kramar, A.; Tinel, N.; Simony-Lafontaine, J. Immunohistochemical assessment of the peripheral benzodiazepine receptor in breast cancer and its relationship with survival. *Clin. Cancer Res.* **2004**, *10*, 2058−2064.

(10) Rechichi, M.; Salvetti, A.; Chelli, B.; Costa, B.; Da Pozzo, E.; Spinetti, F.; Lena, A.; Evangelista, M.; Rainaldi, G.; Martini, C.; Gremigni, V.; Rossi, L. TSPO over-expression increases motility, transmigration and proliferation properties of C6 rat glioma cells. *Biochim. Biophys. Acta* **2008**, *2*, 118−125.

(11) Romeo, E.; Auta, J.; Kozikowski, A. P.; Ma, D.; Papadopoulos, V.; Puia, G.; Costa, E.; Guidotti, A. 2-Aryl-3-indoleacetamides (FGIN-1): a new class of potent and specific ligands for the mitochondrial DBI receptor. *J. Pharmacol. Exp. Ther.* **1992**, *262*, 971−978.

(12) Le Fur, G.; Perrier, M. L.; Vaucher, N.; Imbault, F.; Flamier, A.; Benavides, J.; Uzan, A.; Renault, M. C.; Dubroeucq, C.; Guérémy, C. Peripheral benzodiazepine binding sites: effect of PK 11195, 1-(2-chlorophenyl)-N-methyl-N-(1-methylpropyl)-3-isoquinolinecarboxamide. I. In vitro studies. *Life Sci.* **1983**, *32*, 1839−1847.

(13) Marangos, P. J.; Patel, J.; Boulenger, J. P.; Clark-Rosenberg, R. Characterization of peripheral-type benzodiazepine binding sites in brain using [3H]Ro 5−4864. *Mol. Pharmacol.* **1982**, *22*, 26−32.

(14) Okuyama, S.; Chaki, S.; Yoshikawa, R.; Ogawa, S.; Suzuki, Y.; Okubo, T.; Nakazato, A.; Nagamine, M.; Tomisawa, K. Neuropharmacological profile of peripheral benzodiazepine receptor agonists, DAA1097 and DAA1106. *Life Sci.* **1999**, *64*, 1455−1464.

(15) Denora, N.; Laquintana, V.; Pisu, M. G.; Dore, R.; Murru, L.; Latrofa, A.; Trapani, G.; Sanna, E. 2-Phenyl-imidazo[1,2-a]pyridine compounds containing hydrophilic groups as potent and selective ligands for peripheral benzodiazepine receptors: synthesis, binding affinity and electrophysiological studies. *J. Med. Chem.* **2008**, *51*, 6876−6888.

(16) Trapani, G.; Laquintana, V.; Latrofa, A.; Ma, J.; Reed, K.; Serra, M.; Biggio, G.; Liso, G.; Gallo, J. M. Peripheral Benzodiazepine Receptor Ligand-Melphalan Conjugates for Potential Selective Drug Delivery to Brain Tumors. *Bioconjugate Chem.* **2003**, *14*, 830−839.

(17) Denora, N.; Laquintana, V.; Trapani, A.; Lopedota, A.; Latrofa, A.; Gallo, J. M.; Trapani, G. Translocator protein (TSPO) ligand-Ara-C (cytarabine) conjugates as a strategy to deliver antineoplastic drugs and to enhance drug clinical potential. *Mol. Pharmaceutics* **2010**, *7*, 2255−2269.

(18) Margiotta, N.; Ostuni, R.; Ranaldo, R.; Denora, N.; Laquintana, V.; Trapani, G.; Liso, G.; Natile, G. Synthesis and characterization of a platinum(II) complex tethered to a ligand of the peripheral benzodiazepine receptor. *J. Med. Chem.* **2007**, *50*, 1019−1027.

(19) Margiotta, N.; Denora, N.; Ostuni, R.; Laquintana, V.; Anderson, A.; Johnson, S. W.; Trapani, G.; Natile, G. Platinum(II) complexes with bioactive carrier ligands having high affinity for the translocator protein. *J. Med. Chem.* **2010**, *53*, 5144−5154.

(20) Musacchio, T.; Laquintana, V.; Latrofa, A.; Trapani, G.; Torchilin, V. P. PEG-PE Micelles Loaded with Paclitaxel and Surface-Modified by a PBR-Ligand: Synergistic Anticancer Effect. *Mol. Pharmaceutics* **2009**, *2*, 468−479.

(21) Sekimata, K.; Hatano, K.; Ogawa, M.; Abe, J.; Magata, Y.; Biggio, G.; Serra, M.; Laquintana, V.; Denora, N.; Latrofa, A.; Trapani, G.; Liso, G.; Ito, K. Radiosynthesis and in vivo evaluation of N-[11C]methylated imidazopyridineacetamides as PET tracers for peripheral benzodiazepine receptors. *Nucl. Med. Biol.* **2008**, *35*, 327−334.

(22) Laquintana, V.; Denora, N.; Lopedota, A.; Suzuki, H.; Sawada, M.; Serra, M.; Biggio, G.; Latrofa, A.; Trapani, G.; Liso, G. N-Benzyl-2-(6,8-dichloro-2-(4-chlorophenyl)imidazo[1,2-a]pyridin-3-yl)-N-(6-(7-nitrobenzo[c][1,2,5]oxadiazol-4-ylamino)hexyl)acetamide as a new fluorescent probe for peripheral benzodiazepine receptor and microglial cell visualization. *Bioconjugate Chem.* **2007**, *18*, 1397−1407.

(23) Denora, N.; Laquintana, V.; Trapani, A.; Suzuki, H.; Sawada, M.; Trapani, G. New fluorescent probes targeting the mitochondrial-located translocator protein 18 kDa (TSPO) as activated microglia imaging agents. *Pharm. Res.* **2011**, *28*, 2820−2832.

(24) Piccinonna, S.; Denora, N.; Margiotta, N.; Laquintana, V.; Trapani, G.; Natile, G. Synthesis, Characterization, and Binding to the Translocator Protein (18 kDa, TSPO) of a New Rhenium Complex as a Model of Radiopharmaceutical Agents. *Z. Anorg. Allg. Chem.* **2013**, *636*, 1606−1612.

(25) Laquintana, V.; Denora, N.; Musacchio, T.; Lasorsa, M.; Latrofa, A.; Trapani, G. Peripheral benzodiazepine receptor ligand-PLGA polymer conjugates potentially useful as delivery systems of apoptotic agents. *J. Controlled Release* **2009**, *137*, 185−195.

(26) Denora, N.; Cassano, T.; Laquintana, V.; Lopalco, A.; Trapani, A.; Cimmino, C. S.; Laconca, L.; Giuffrida, A.; Trapani, G. Novel

codrugs with GABAergic activity for dopamine delivery in the brain. *Int. J. Pharmaceutics* **2012**, *437*, 221−231.
(27) Denora, N.; Laquintana, V.; Lopalco, A.; Iacobazzi, R. M.; Lopedota, A.; Cutrignelli, A.; Iacobellis, G.; Annese, C.; Cascione, M. F.; Leporatti, S.; Franco, M. In vitro targeting and imaging the translocator protein TSPO 18-kDa through G(4)-PAMAM−FITC labeled dendrimer. *J. Controlled Release* **2013**, *172*, 1111−1125.
(28) Bocci, G.; Danesi, R.; Di Paolo, A. D.; Innocenti, F.; Allegrini, G.; Falcone, A.; Melosi, A.; Battistoni, M.; Barsanti, G.; Conte, P. F.; Del Tacca, M. Comparative Pharmacokinetic Analysis of 5-Fluorouracil and Its Major Metabolite 5-Fluoro-5,6-dihydrouracil after Conventional and Reduced Test Dose in Cancer Patients. *Clin. Cancer Res.* **2000**, *6*, 3032−3037.
(29) Lu, X. Y.; Zhang, Y.; Wang, L. Preparation and In Vitro Drug-Release Behavior of 5-Fluorouracil-Loaded Poly(hydroxybutyrate-*co*-hydroxyhexanoate) Nanoparticles and Microparticles. *J. Appl. Polym. Sci.* **2010**, *116*, 2944−2950.
(30) Sastre, R. L.; Olmo, R.; Teijón, C.; Muñíz, E.; Teijón, J. M.; Blanco, M. D. 5-Fluorouracil plasma levels and biodegradation of subcutaneously injected drug-loaded microspheres prepared by spray-drying poly(D,L-lactide) and poly(D,L-lactide-*co*-glycolide) polymers. *Int. J. Pharmaceutics* **2007**, *338*, 180−190.
(31) Fournier, E.; Passirani, C.; Colin, N.; Breton, P.; Sagodira, S.; Benoit, J. P. Development of novel 5-FU-loaded poly(methylidene malonate 2.1.2)-based microspheres for the treatment of brain cancers. *Eur. J. Pharm. Biopharm.* **2004**, *57*, 189−97.
(32) Menei, P.; Jadaud, E.; Faisant, N.; Boisdron-Celle, M.; Michalak, S.; Fournier, D.; Delhaye, M.; Benoit, J. P. Stereotaxic implantation of 5-fluorouracil-releasing microspheres in malignant glioma. *Cancer* **2004**, *100*, 405−410.
(33) Menei, P.; Boisdron-Celle, M.; Croué, A.; Guy, G.; Benoit, J. P. Effect of stereotactic implantation of biodegradable 5-fluorouracil-loaded microspheres in healthy and C6 glioma-bearing rats. *Neurosurgery* **1996**, *39*, 117−123.
(34) Murakami, H.; Kobayashi, M.; Takeuchi, H.; Kawashima, Y. Preparation of poly(DL-lactide-*co*-glycolide) nanoparticles by modified spontaneous emulsification solvent diffusion method. *Int. J. Pharmaceutics* **1999**, *187*, 143−152.
(35) Cohen-Sela, E.; Chorny, M.; Koroukhov, N.; Danenberg, H. D.; Golomb, G. A new double emulsion solvent diffusion technique for encapsulating hydrophilic molecules in PLGA nanoparticles. *J. Controlled Release* **2009**, *133*, 90−95.
(36) Chou, T. C.; Talalay, P. Quantitative analysis of dose-effect relationships: the combined effects of multiple drugs or enzyme inhibitors. *Adv. Enzyme Regul.* **1984**, *22*, 27−55.
(37) Olson, J. M.; Mcneel, W.; Young, A. B.; Mancini, W. R. Localization of the Peripheral-Type Benzodiazepine Binding-Site to Mitochondria of Human Glioma-Cells. *J. Neurooncol.* **1992**, *13*, 35−42.
(38) Mundargi, R. C.; Babu, V. R.; Rangaswamy, V.; Patel, P.; Aminabhavi, T. M. Nano/micro technologies for delivering macromolecular therapeutics using poly(D,L-lactide-co-glycolide) and its derivatives. *J. Controlled Release* **2008**, *125*, 193−209.
(39) Lu, X. Y.; Zhang, Y.; Wang, L. Preparation and In Vitro Drug-Release Behavior of 5-Fluorouracil-Loaded Poly(hydroxybutyrateco-hydroxyhexanoate) Nanoparticles and Microparticles. *J. Appl. Polym. Sci.* **2010**, *116*, 2944−2950.
(40) Nair, K. L.; Jagadeeshan, S.; Nair, S. A.; Kumar, G. S. Biological evaluation of 5-fluorouracil nanoparticles for cancer chemotherapy and its dependence on the carrier, PLGA. *Int. J. Nanomed.* **2011**, *6*, 1685−1697.
(41) Dinarvand, R.; Sepehri, N.; Manoochehri, S.; Rouhani, H.; Atyabi, F. Polylactide-co-glycolide nanoparticles for controlled delivery of anticancer agents. *Int. J. Nanomed.* **2011**, *6*, 877−895.
(42) Laquintana, V.; Trapani, A.; Denora, N.; Wang, F.; Gallo, J. M.; Trapani, G. New strategies to deliver anticancer drugs to brain tumors. *Expert Opin Drug Deliv.* **2009**, *6*, 1017−1032.
(43) Liu, Y.; Lu, W. Recent advances in brain tumor-targeted nano-drug delivery systems. *Expert Opin. Drug Delivery* **2012**, *9*, 671−686.